

LHC constraints on hidden gravitons

J. A. R. Cembranos^{1a} R. L. Delgado^{2b} H. Villarrubia-Rojo^{3c}

^a*Departamento de Física Teórica and Instituto de Física de Partículas y del Cosmos IPARCOS, Universidad Complutense de Madrid, E-28040 Madrid, Spain*

^b*Departamento de Matemática Aplicada a las TIC, ETSIST, Universidad Politécnica de Madrid, E-28040 Madrid, Spain; Technische Universität München, Physik-Department T30f, James-Frank-Str. 1, 85748 Garching, Germany; INFN-Firenze, via G. Sansone, 1, 50019 Sesto Fiorentino (FI), Italia*

^c*Institute for Theoretical Physics, ETH Zürich, Wolfgang-Pauli-Strasse 27, 8093, Zürich, Switzerland*

ABSTRACT: We analyze LHC data in order to constrain the parameter space of new spin-2 particles universally coupled to the energy-momentum tensor. These new hypothetical particles are the so-called hidden gravitons, whose phenomenology at low energies is determined by two parameters: its mass and its dimensional coupling constant. Hidden gravitons arise in many different extensions of the Standard Model of particles and interactions and General Relativity. Their phenomenology has been studied mainly in relation to modifications of gravity and astrophysical signatures. In this work, we extend the constraints for heavy hidden gravitons, with masses larger than 1 GeV, by taking into account events collected by ATLAS and CMS in the WW channel, Drell-Yan processes, and the diphoton channel from proton–proton collisions at $\sqrt{s} = 8$ TeV.

¹cembra@ucm.es

²rafael.delgado@upm.es

³herojo@phys.ethz.ch

Contents

| | | |
|----------|--------------------------------|----------|
| 1 | Introduction | 1 |
| 2 | Theoretical framework | 2 |
| 3 | Data analysis | 3 |
| 4 | Summary and conclusions | 5 |

1 Introduction

The beginning of the 21st century has witnessed the consolidation of two standard models in fundamental physics: the Standard Model (SM) of particle physics and the Λ CDM model of cosmology. Both models have withstood many tests over the years and are supported by a large number of extremely precise measurements and observations. Taken together, these two leading models constitute a baseline of our understanding of the Universe. However, while their success cannot be contested, many questions still remain.

Most of the questions that have prompted the search for extensions to the standard paradigm are theoretical in nature: CP problem, origin of neutrino masses, fundamental nature of dark matter and dark energy,... Also, as the precision of experiments and observations increase, new puzzles may arise from the observational side, as can be illustrated by the growing concern in the cosmological community over the so-called H_0 tension [1, 2].

Traditionally, the interplay between particle physics and cosmology has proven to be extremely fruitful. Many beyond-SM (BSM) models can be tested based on their cosmological implications, e.g. the QCD axion can simultaneously solve the CP problem [3–5] and act as dark matter [6, 7]. Similarly, new advances in cosmology can also shed new light on particle physics, e.g. large-scale structure surveys expect to measure, at least, the sum of the neutrino masses. Hence, the observational implications of any beyond-SM or beyond- Λ CDM model should be carefully analyzed in both realms.

From the QCD axion to modified gravity theories like Horndeski [8–10] and Generalized Proca [10–12], the vast majority of extensions to the standard paradigm rely on the inclusion of additional scalar or vector fields, i.e. new spin 0 and 1 particles. Tensor fields, i.e. spin-2 particles, on the other hand, are commonly overlooked. This choice seems reasonable on the grounds of simplicity but not on the grounds of naturalness. Since we believe that fundamental spin-2 particles also exist in Nature and mediate gravitational interactions, i.e. gravitons, we must also explore extensions based on spin-2 fields.

While comparatively less studied in the literature, new massive spin-2 degrees of freedom have been shown to arise in different modifications of gravity. Extradimensional theories of gravity, like the ADD [13–15] and Randall-Sundrum [16–19] models, generically

predict the existence of new massive spin-2 particles, either with a continuum mass spectrum or as a number of widely separated mass resonances. Also in the context of bimetric theories of gravity [20–22] a new massive spin-2 degree of freedom naturally appears.

The possible existence of new massive gravitons, that we will generically refer to as hidden gravitons, prompts the question: what would their observational signature be? This question was partially answered in [23], where different constraints on the mass and coupling of the hidden gravitons were derived, based on their effects on fifth-force tests and on stellar energy-loss arguments. In this work we will extend these findings to higher masses, where the astrophysical probes are not competitive and the signatures in particle colliders set the most restrictive bounds. Similar searches were performed in [24–26] for specific models and with less updated data.

This work is structured as follows. In section 2 we present the details on the theoretical model and the implementation. Section 3 contains a description of the different experimental channels and the constraints on the model. Finally, in section 4 we summarize the main conclusions of the work and show the combined experimental bounds on the hidden gravitons.

2 Theoretical framework

We will use a generic framework to describe the massive graviton

$$\mathcal{L}_h \equiv -\frac{1}{2}\partial^\alpha h^{\mu\nu}(\partial_\alpha h_{\mu\nu} - 2\partial_{(\mu}h_{\nu)\alpha} - \partial_\alpha h\eta_{\mu\nu} + 2\partial_{(\mu}h\eta_{\nu)\alpha}) - \frac{1}{2}m^2(h_{\mu\nu}^2 - h^2), \quad (2.1)$$

where m is the graviton mass and $\eta_{\mu\nu}$ is the Minkowski metric. This Lagrangian is the well-known Fierz-Pauli Lagrangian [27] that describes a massive spin-2 particle. The kinetic and mass terms in this Lagrangian can be found imposing the absence of ghost instabilities [10, 28]. This is the general linear description of a massive spin-2 particle, so it can be used as a generic framework to study theories with spin-2 degrees of freedom. We will also choose a universal coupling to the SM for the hidden gravitons, like the standard massless gravitons,

$$\mathcal{L} = \mathcal{L}_{\text{SM}} + \mathcal{L}_h + \kappa h_{\mu\nu} T_{\text{SM}}^{\mu\nu}, \quad (2.2)$$

where κ is the universal coupling to the Standard Model, that can be also rewritten as $\kappa = 1/M_h = \sqrt{8\pi G_h}$.

The relevant parton level amplitudes for the subprocesses are $q\bar{q} \rightarrow gG$, $qg \rightarrow qG$ and $gg \rightarrow gG$, where the letters q and g refer generally to quarks and gluons, whereas the G letter stands for the hidden graviton. The corresponding cross sections have been studied in different contexts. For example, they can be found on [24], but for the shake of clarity we reproduce them here:

$$\frac{d\sigma(q\bar{q} \rightarrow gG)}{dt} = \frac{\alpha_s \kappa^2}{36s} F_1(t/s, m^2/s), \quad (2.3)$$

$$\frac{d\sigma(qg \rightarrow qG)}{dt} = \frac{\alpha_s \kappa^2}{96s} F_2(t/s, m^2/s), \quad (2.4)$$

$$\frac{d\sigma(gg \rightarrow gG)}{dt} = \frac{3\alpha_s \kappa^2}{16s} F_3(t/s, m^2/s); \quad (2.5)$$

where s , t and u are the usual Mandelstam variables for a $2 \rightarrow 2$ scattering process. The functions F_1 , F_2 and F_3 are defined by

$$x(y-1-x)F_1(x,y) = (1+4x)y^3 - 6x(1+2x)y^2 + (1+6x+18x^2+16x^3)y - 4x(1+x)(1+2x+2x^2), \quad (2.6)$$

$$x(y-1-x)F_2(x,y) = -2y^4 + 4(1+x)y^3 - 3(1+4x+x^2)y^2 + (1+x)(1+8x+x^2)y - 4x(1+x^2), \quad (2.7)$$

$$x(y-1-x)F_3(x,y) = y^4 - 2(1+x)y^3 + 3(1+x^2)y^2 - 2(1+x^3)y + 1 + 2x + 3x^2 + 2x^3 + x^4. \quad (2.8)$$

3 Data analysis

For the computation of the LHC constraints, Pythia 8 [29, 30], DELPHES [31] and RIVET [32, 33] are used. We rely on several *validated* RIVET [32, 33] analysis for comparison with experimental data. The BSM processes $gg \rightarrow gG$, $qg \rightarrow qG$ and $q\bar{q} \rightarrow gG$ are implemented as parton level processes inside Pythia 8 framework. We take advantage of the fact that Pythia 8 is implemented as an object oriented C++ library. Hence, the new processes are implemented by inheritance of the `Sigma2Process` class, without modifying the library.

In order to constrain the parameters of the model, we study three observational channels: $H \rightarrow WW$ [34], Drell-Yan [35] and diphoton [36]. Each of them is detailed below. Given that all the previous data is compatible with the SM, we will just try to ascertain whether the remaining uncertainty in the observations leave room for the simulated signal. We perform a χ^2 test, assuming that the SM background can approximately account for the observed data, and then estimating the error as a quadratic sum of the uncertainties in the data and the signal. For the computations, we used 175.000h of computer time granted on C2PAP supercomputing facility at the Leibniz Supercomputing Center. Each point in the m vs. κm plots represents 200.000 events generated on Pythia. These events were further processed on Rivet.

The first process that we study is the decay H to WW , using the CMS_2017_I1467451 RIVET analysis (Fig. 1a). It models the CMS study [34], based on $H \rightarrow WW$ decay channel at $\sqrt{s} = 8$ TeV (integrated luminosity of 19.4 fb^{-1}), on the leptonic channel $H \rightarrow W^+W^- \rightarrow 2l2\nu$. The lepton transverse momentum $p_T(ll)$ and missing transverse momentum $p_{T,\text{miss}}$ are used to reconstruct the Higgs transverse momentum $p_T(H)$. The main cuts are: leading lepton, $P_T > 20$ GeV; subleading lepton, $P_T > 10$ GeV; pseudorapidity of electrons and muons, $|\eta| < 2.5$; invariant mass of the two charged leptons, $m_{ll} > 12$ GeV; charged lepton pair, $p_T > 30$ GeV; transverse invariant mass of the leptonic system, $m_T^{e\mu\nu\nu} > 50$ GeV.

The second channel that we consider in this work is based on the RIVET analysis ATLAS_2016_I1467454 (Fig. 1b). This is a Drell-Yan study in ATLAS [35], $Z/\gamma^* \rightarrow l^+l^-$ and photo-induced $\gamma\gamma \rightarrow l^+l^-$. Integrated luminosity of 20.3 fb^{-1} at $\sqrt{s} = 8$ TeV. For both the electron and muon channels, the cut over the invariant mass of the lepton pairs

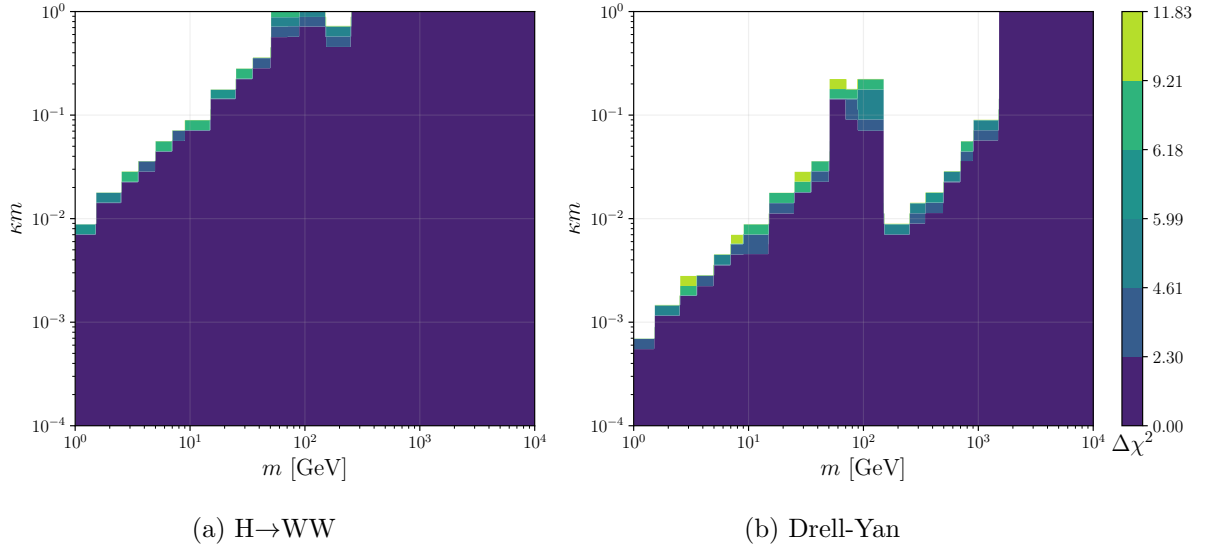


Figure 1: Density plots for the $H \rightarrow WW$ process in CMS (left) and Drell-Yan in ATLAS (right). The white region is excluded.

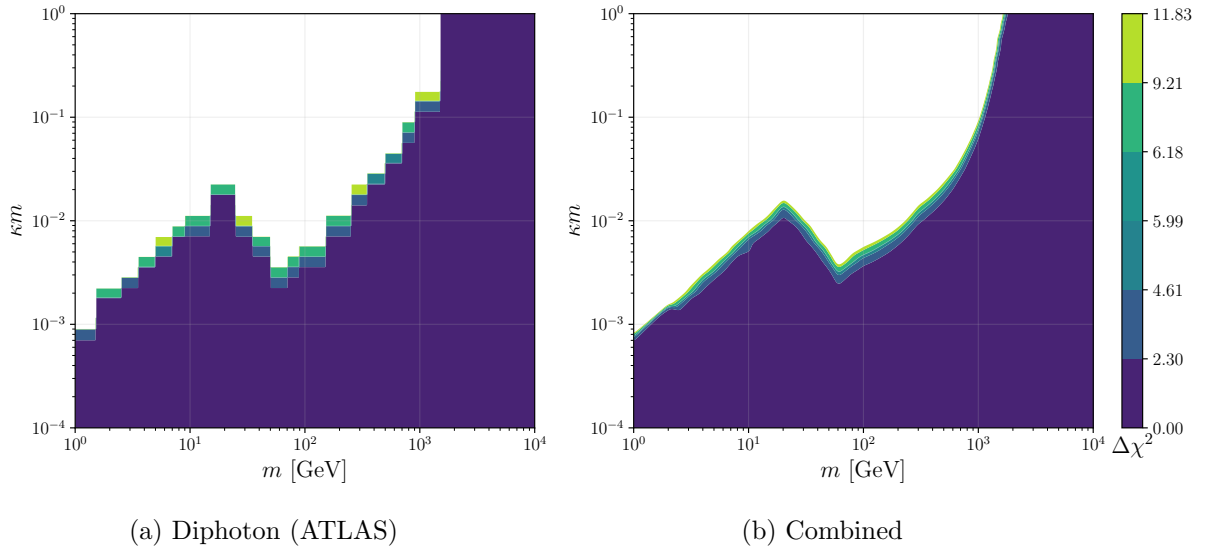


Figure 2: Density plots for the diphoton production in ATLAS (left) and combined density plot for the three channels (right). The white region is excluded.

is $116 \text{ GeV} < m_{ll} < 1500 \text{ GeV}$. The electron channel has a cut of $E_T(e) > 40 \text{ GeV}$ for the leading electron and $E_T(e) > 30 \text{ GeV}$ for the subleading one. The pseudorapidities are in the range $|\eta^e| < 2.47$, excluding $1.37 < |\eta^e| < 1.52$. The absolute difference in pseudorapidity between the two electrons is restricted to $|\Delta\eta_{ee}| < 3.5$. Concerning the muon channel, at least two oppositely charged muones with transverse momenta $p_T^\mu > 40 \text{ GeV}$ (leading muon) and $p_T^\mu > 30 \text{ GeV}$ (subleading muon) are required. The pseudorapidity should be $|\eta^\mu| < 2.4$. No requirement is placed on $\Delta\eta_{\mu\mu}$.

Finally, we also include the RIVET analysis ATLAS_2017_I1591327 (Fig. 2a), that corresponds to the diphoton production in ATLAS [36] at $\sqrt{s} = 8 \text{ TeV}$ and integrated luminosity of 20.2 fb^{-1} . The cuts are: transverse energies $E_{T,1}^\gamma > 40 \text{ GeV}$ (leading photon) and $E_{T,2}^\gamma > 30 \text{ GeV}$ (subleading one) and pseudorapidities $|\eta^\gamma| < 1.37$ or $1.56 < |\eta^\gamma| < 2.37$.

The combined constraints from the three processes can be found on Fig. 2b. On Fig. 3 we compare these new collider constraints on hidden gravitons with those of astrophysical and 5th force tests [23].

4 Summary and conclusions

The results of the commented analyses are translated into exclusion limits on the mass and the coupling of the hidden graviton. The sensitivity of the constraints are limited by the effect of experimental uncertainties related to jet and transverse missing energy scales and resolutions. The choice of different PDF sets results in up to $\sim 10\%$ order of magnitude uncertainties in the acceptance and in the cross section. Varying the renormalization and factorization scales introduces $\sim 5\%$ variations of the cross section and acceptance. In addition, the uncertainty in the integrated luminosity is included. Fig. 1 shows the derived 95% CL exclusion limits in the mentioned $\kappa - m$ parameter space of the hidden gravitons for the WW channel (left panel) and Drell-Yan process (right panel). The same bounds are plotted for the diphoton channel in Fig. 2 (left panel). The combined results from the tree analyses are shown in Fig. 2 (right panel). These combined constraints are dominated by the diphoton data.

These results are translated into the general parameter space of hidden gravitons presented in Fig. 3, where it is possible to see that they are the most constraining for heavy gravitons, i.e. for hidden graviton masses larger than $m \sim 1 \text{ GeV}$. The phenomenology of gravitons with masses between $m \sim 1 \text{ eV}$ and $m \sim 1 \text{ GeV}$ is more limited by astrophysical data [23], whereas light hidden gravitons ($m \lesssim 1 \text{ eV}$) suffer important restrictions from fifth force experiments [23].

In summary, results are reported from a search for hidden gravitons in events associated with the WW channel, Drell-Yan processes, and the diphoton channel from proton-proton collisions at $\sqrt{s} = 8 \text{ TeV}$ at the LHC, based on data corresponding to an integrated luminosity close to 20 fb^{-1} collected by the ATLAS (Drell-Yan and diphoton) and CMS (WW) experiments. The measurements are in agreement with the SM predictions. The results are translated into model-independent 95% confidence-level limits on the universal hidden graviton coupling depending on its mass. The comparison with previous analyses shows that the constraints derived in this study are the most important for heavy hidden gravitons.

Acknowledgments

We would like to thank Antonio López Maroto for valuable discussions at the beginning of this study. R.L.D. was financially supported by the Ramón Areces Foundation, the

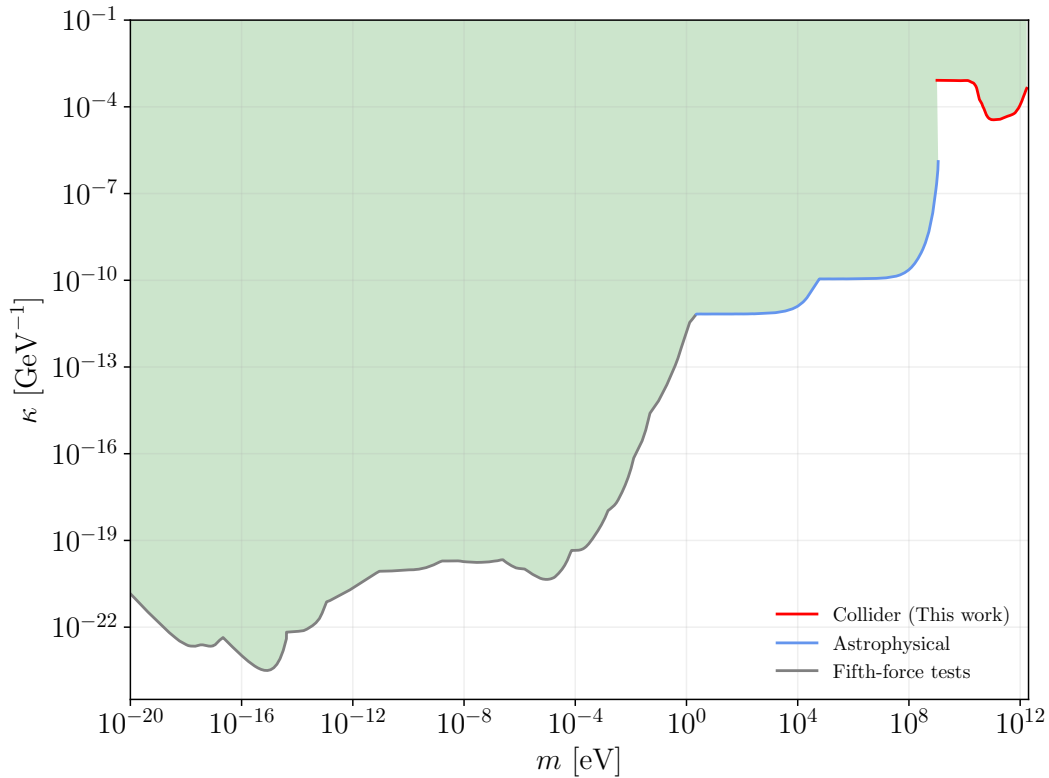


Figure 3: Total constraints in the hidden-graviton parameter space. The shaded region is excluded. “Fifth-force tests” represents a collection of laboratory and Solar System experiments, see [23] and references therein. The astrophysical bounds were derived in [23], based on stellar energy-loss arguments. “Collider” represents the combined bounds from Figures 1 and 2.

INFN post-doctoral fellowship AAOODGF-2019-0000329 and the Spanish grant MICINN: PID2019-108655GB-I00. HVR is supported by funding from the European Research Council (ERC) under the European Unions Horizon 2020 research and innovation programme grant agreement No 801781. The simulations have been carried out on the computing facilities of the Computational Center for Particle and Astrophysics (C2PAP) and the Leibniz Supercomputing Center (SuperMUC), on the local theory cluster (T30 cluster) of the Physics Department of the Technische Universität München (TUM), and on local computing facilities at the INFN-Firenze.

References

- [1] J. L. Bernal, L. Verde and A. G. Riess, *The trouble with H_0* , *JCAP* **10** (2016) 019.
- [2] L. Verde, T. Treu and A. G. Riess, *Tensions between the Early and the Late Universe*, *Nature Astron.* **3** (2019) 891.
- [3] R. D. Peccei and H. R. Quinn, *CP Conservation in the Presence of Instantons*, *Phys. Rev. Lett.* **38** (1977) 1440.

- [4] F. Wilczek, *Problem of Strong P and T Invariance in the Presence of Instantons*, *Phys. Rev. Lett.* **40** (1978) 279.
- [5] S. Weinberg, *A New Light Boson?*, *Phys. Rev. Lett.* **40** (1978) 223.
- [6] P. Sikivie and Q. Yang, *Bose-Einstein Condensation of Dark Matter Axions*, *Phys. Rev. Lett.* **103** (2009) 111301.
- [7] D. J. E. Marsh, *Axion Cosmology*, *Phys. Rept.* **643** (2016) 1.
- [8] G. W. Horndeski, *Second-order scalar-tensor field equations in a four-dimensional space*, *Int. J. Theor. Phys.* **10** (1974) 363.
- [9] C. Deffayet, G. Esposito-Farese and A. Vikman, *Covariant Galileon*, *Phys. Rev. D* **79** (2009) 084003.
- [10] L. Heisenberg, *A systematic approach to generalisations of General Relativity and their cosmological implications*, *Phys. Rept.* **796** (2019) 1.
- [11] L. Heisenberg, *Generalization of the Proca Action*, *JCAP* **05** (2014) 015.
- [12] J. Beltran Jimenez and L. Heisenberg, *Generalized multi-Proca fields*, *Phys. Lett. B* **770** (2017) 16.
- [13] N. Arkani-Hamed, S. Dimopoulos and G. R. Dvali, *The Hierarchy problem and new dimensions at a millimeter*, *Phys. Lett.* **B429** (1998) 263.
- [14] I. Antoniadis, N. Arkani-Hamed, S. Dimopoulos and G. R. Dvali, *New dimensions at a millimeter to a Fermi and superstrings at a TeV*, *Phys. Lett.* **B436** (1998) 257.
- [15] N. Arkani-Hamed, S. Dimopoulos and G. R. Dvali, *Phenomenology, astrophysics and cosmology of theories with submillimeter dimensions and TeV scale quantum gravity*, *Phys. Rev.* **D59** (1999) 086004.
- [16] L. Randall and R. Sundrum, *A large mass hierarchy from a small extra dimension*, *Phys. Rev. Lett.* **83** (1999) 3370.
- [17] L. Randall and R. Sundrum, *An alternative to compactification*, *Phys. Rev. Lett.* **83** (1999) 4690.
- [18] H. Davoudiasl, J. Hewett and T. Rizzo, *Phenomenology of the Randall-Sundrum Gauge Hierarchy Model*, *Phys. Rev. Lett.* **84** (2000) 2080.
- [19] J. Garriga and T. Tanaka, *Gravity in the brane world*, *Phys. Rev. Lett.* **84** (2000) 2778.
- [20] S. F. Hassan and R. A. Rosen, *On Non-Linear Actions for Massive Gravity*, *JHEP* **07** (2011) 009.
- [21] A. Schmidt-May and M. von Strauss, *Recent developments in bimetric theory*, *J. Phys.* **A49** (2016) 183001.
- [22] C. García-García, A. L. Maroto and P. Martín-Moruno, *Cosmology with moving bimetric fluids*, *JCAP* **1612** (2016) 022.
- [23] J. A. R. Cembranos, A. L. Maroto and H. Villarrubia-Rojo, *Constraints on hidden gravitons from fifth-force experiments and stellar energy loss*, *JHEP* **09** (2017) 104.
- [24] G. F. Giudice, R. Rattazzi and J. D. Wells, *Quantum gravity and extra dimensions at high-energy colliders*, *Nucl. Phys.* **B544** (1999) 3.

- [25] P. de Aquino, K. Hagiwara, Q. Li and F. Maltoni, *Simulating graviton production at hadron colliders*, *JHEP* **06** (2011) 132.
- [26] Y. Tang, *Implications of LHC Searches for Massive Graviton*, *JHEP* **08** (2012) 078.
- [27] M. Fierz and W. Pauli, *On relativistic wave equations for particles of arbitrary spin in an electromagnetic field*, *Proc. Roy. Soc. Lond.* **A173** (1939) 211.
- [28] C. de Rham, *Massive Gravity*, *Living Rev. Rel.* **17** (2014) 7.
- [29] T. Sjostrand, S. Mrenna and P. Z. Skands, *PYTHIA 6.4 Physics and Manual*, *JHEP* **05** (2006) 026.
- [30] T. Sjostrand, S. Mrenna and P. Z. Skands, *A Brief Introduction to PYTHIA 8.1*, *Comput. Phys. Commun.* **178** (2008) 852.
- [31] DELPHES 3 collaboration, *DELPHES 3, A modular framework for fast simulation of a generic collider experiment*, *JHEP* **02** (2014) 057.
- [32] A. Buckley, J. Butterworth, L. Lonnblad, D. Grellscheid, H. Hoeth, J. Monk et al., *Rivet user manual*, *Comput. Phys. Commun.* **184** (2013) 2803.
- [33] C. Bierlich et al., *Robust Independent Validation of Experiment and Theory: Rivet version 3*, *SciPost Phys.* **8** (2020) 026.
- [34] CMS collaboration, *Measurement of the transverse momentum spectrum of the Higgs boson produced in pp collisions at $\sqrt{s} = 8$ TeV using $H \rightarrow WW$ decays*, *JHEP* **03** (2017) 032.
- [35] ATLAS collaboration, *Measurement of the double-differential high-mass Drell-Yan cross section in pp collisions at $\sqrt{s} = 8$ TeV with the ATLAS detector*, *JHEP* **08** (2016) 009.
- [36] ATLAS collaboration, *Measurements of integrated and differential cross sections for isolated photon pair production in pp collisions at $\sqrt{s} = 8$ TeV with the ATLAS detector*, *Phys. Rev. D* **95** (2017) 112005.